International Journal of Scientific Research in Engineering and Management (IJSREM)
Volume: 09 Issue: 06 | June - 2025 SJIF Rating: 8.586 ISSN: 2582-3930

Hardware Implementation of Improved Voltage Gain by Hybrid Non-Isolated Bidirectional Dc-Dc Converter

ARAVIND KUMARAN R[1], GEETHA V[2]

[1]PG Student, ME (Power Electronics and Drives), Government College of Engineering, Salem.

[2] Professor and Head, EEE Department, Government College of Engineering, Salem

---

Abstract - This work presents the design and analysis of a Hybrid Non-Isolated Bidirectional DC-DC Converter (HNB-DC), specifically developed for electric vehicle (EV) charging and discharging applications interfaced with a DC grid. The proposed converter topology addresses limitations in conventional designs by incorporating a bidirectional power flow capability, enabling efficient energy transfer between the grid and EV batteries. To achieve a high voltage conversion ratio suitable for EV applications, the converter utilizes an enhanced buck-boost architecture featuring four active switches with corresponding diodes, two inductors, and a capacitor. This configuration supports improved energy storage and transfer efficiency, making it a suitable candidate for practical EV charging stations. The design is validated through extensive simulations conducted in MATLAB/SIMULINK using optimized parameters, confirming its effectiveness in delivering high-performance voltage conversion and bidirectional energy flow. This study lays the groundwork for hardware implementation and experimental verification of the proposed converter for real-world EV infrastructure.

***Key Words*:** Bidirectional, Hybrid, Voltage Gain

1.INTRODUCTION

The global push toward sustainability and reduced environmental impact has significantly increased the adoption of Green Energy Sources (GES), such as solar and wind power. These renewable sources are instrumental in minimizing carbon emissions and ecological footprints. However, the inherent intermittency and unpredictability of GES input power present challenges in matching energy generation with consumer demand, thereby affecting the stability and reliability of the electrical grid.

To mitigate these challenges, autonomous renewable energy systems are increasingly integrated with energy storage solutions—such as supercapacitors, batteries, and other buffering components—that ensure continuous and reliable operation under varying load conditions. These systems are now widely employed across residential, commercial, and industrial sectors for lighting, heating, and powering electronic appliances.

Concurrently, the urgency to reduce reliance on fossil fuels—driven by the escalating concerns of global warming and environmental degradation—has propelled substantial growth in the Electric Vehicle (EV) industry. A critical component enabling the integration of renewable energy sources (RES) and EV infrastructure is the **Bidirectional DC–DC Converter**. This converter facilitates energy transfer from RES to storage devices (charging mode) and from storage to the load or grid (discharging mode), enabling dynamic and efficient power management.

Bidirectional DC–DC converters are essential in systems requiring two-way power flow, supporting applications such as vehicle-to-grid (V2G), load management, and backup power systems. By combining elements of buck, boost, and buck-boost topologies, hybrid converters achieve improved efficiency, wider voltage gain, and reduced stress on individual components. These advantages make hybrid, non-isolated topologies highly suitable for EV and green energy systems, especially where cost, size, and reliability are critical.

Non-isolated hybrid topologies, including multi-level, switched-capacitor, CUK/CUK, SEPIC/ZETA, and coupled-inductor variants, offer a wide range of operational flexibility. However, configurations like multi-level or switched-capacitor designs may require additional switches and capacitors to achieve high voltage gains, often leading to increased circuit complexity.

In this context, a Hybrid Non-Isolated Bidirectional DC–DC Converter is developed and analyzed for both software simulation and hardware implementation. This design aims to provide a compact, efficient, and robust solution for managing bidirectional power flow in renewable-powered EV charging systems. The converter's performance is first validated through detailed simulations in MATLAB/SIMULINK using practical operating parameters. Subsequently, a hardware prototype is developed to verify the simulated results under real-world conditions, demonstrating the system's feasibility and effectiveness for modern green energy applications.

2. OBJECTIVE

The objective of this paper is to design and implement a Hybrid Non-Isolated Bidirectional DC-DC Converter that addresses the limitations of conventional single-stage converters—such as limited voltage gain, low efficiency, and high component stress—through improved topology and control. This hardware implementation aims to: Support a wide range of input and output voltage levels to accommodate diverse applications, including battery charging, electric vehicles (EVs), and renewable energy systems. Enhance overall efficiency by minimizing power losses caused by resistive elements in semiconductor devices. Reduce electrical and thermal stress on passive components and switching devices, thereby improving their reliability and extending system lifespan. Optimize switching patterns and distribute voltage and current stresses across multiple components to improve thermal management and prevent overheating. Achieve higher voltage conversion ratios with reduced component count and complexity compared to traditional converters. Through practical hardware realization and testing, the converter's effectiveness in real-world operating conditions will be demonstrated, validating its suitability for next-generation green energy and EV infrastructure.

3. PROPOSED SYSTEM

HYBRID DC-DC CONVERTER

A promising method for successfully overcoming the obstacles is the use of hybrid DC–DC converters. Multiple converter topologies or approaches are combined in hybrid DC–DC converters to accomplish particular performance goals. These hybrid solutions maximize efficiency, voltage regulation, power density, and other required attributes by combining the benefits of various converter types.

Table 1 Hybrid DC-DC Converters and Topologies

HYBRID DC-DC CONVERTER	TOPOLOGIES COMBINED
Buck-Boost Converter	Buck, Boost
SEPIC-Cuk Converter	SEPIC, Cuk
Flyback-Forward Converter	Flyback, forward
Full-Bridge LLC Converter	Full-Bridge, LLC
Hybrid Multilevel Converter	Various multilevel topologies
Flyback-Cuk Converter	Flyback, CuK
Flyback-SEPIC Converter	Flyback, SEPIC

BIDIRECTIONAL DC-DC CONVERTER

A bidirectional converter is a power electronic device that can facilitate the flow of electrical power in both directions. Unlike traditional unidirectional converters, which only allow power to flow in one direction, bidirectional converters offer flexibility and efficiency in various applications. By strategically controlling the switching patterns of the power electronic devices, the converter can either step up or step down the voltage, or even reverse the direction of power flow. Bidirectional converters enable the charging of the vehicle's battery from the grid and also allow the vehicle to feed power back to the grid (vehicle-to-grid, or V2G). They enable the charging and discharging of batteries, optimizing energy storage and utilization.

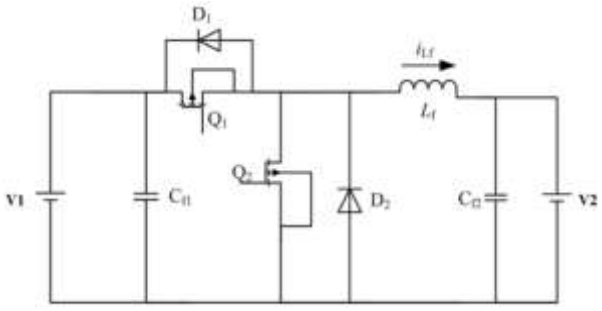

Figure 1 Basic Circuit of Bidirectional DC-DC Converter

Bidirectional DC–DC converters are available in two configurations: isolated topology and non-isolated topology. Magnetic isolation separates the power transfer between the input and output in an isolated topology. Non-isolated topology, on the other hand, does not involve isolation. The non-isolated conventional bidirectional DC–DC converter's primary and simplest topology is the buck–boost bidirectional converter. When charging the storage systems, the converter runs in buck mode. When discharging electricity to meet the DC/DC voltage needs, it functions in boost mode.

CIRCUIT DIAGRAM

Figure 2 displays the converter's anticipated topology. It has two inductors, a capacitor, and four power switches with body diodes. In these works, two inductors with different values are implemented, resulting in differing currents when compared to the inductor value in the converter. During step-up operation, the two boost converters created by this topology's two inductors increase their voltage gain. The current in one of the switches is simultaneously the high sum of the two inductor currents during step-down operation. The relevant switch's switching losses are significantly decreased by employing synchronous rectification, which raises efficiency.

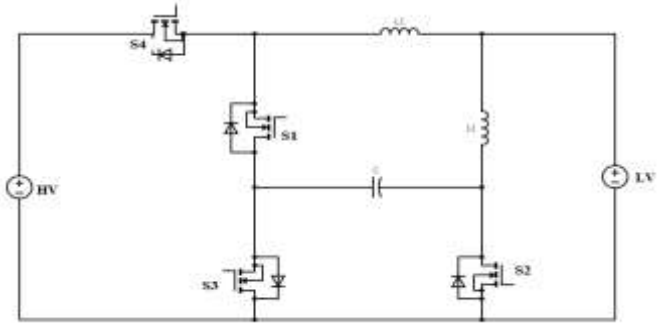

Figure 2 Circuit Diagram of Proposed System

The steady-state analysis for the boost and buck modes of operation have been conducted under the following presumptions. The equivalent series resistance of the inductors and capacitor is disregarded for the ON-state resistance RDS (ON) of the power switches, and the voltage across the capacitor is taken to be constant. The switches S_3 and S_4 are controlled simultaneously using the pulse width modulation (PWM) technique. The S_1 and S_2 switches function as synchronous rectifiers.

MODES OF OPERATION

There are two modes of operation in this proposed system. They are

1. Step – Down Operation
2. Step – Up Operation

STEP – DOWN OPERATION

Figure 3 shows the circuit of the proposed topology in step-down operation; S1 and S2 serve as synchronous rectifiers and S3 and S4 as control switches. Depending on when the associated switches are triggered, it can operate in two different states.

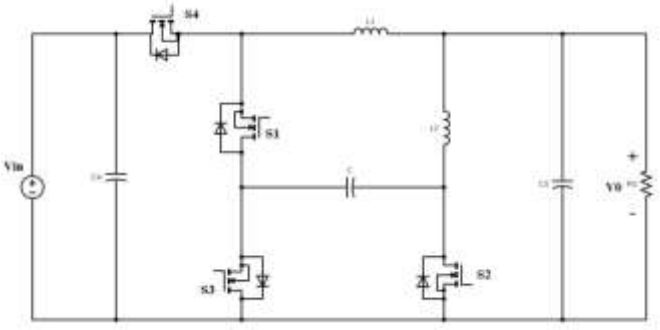

Figure 3 Step-Down Operation

STATUS – I ($t_0 \leq t \leq t_1$)

During this time span, the switches S_3 and S_4 are turned ON, while the switches S_1 and S_2 turned OFF at the same time by means of applying the gate pulses to the appropriate switches. The energy from the high-voltage end, which is the input voltage V_{in}, is transferred on the way to the inductor L_1.The capacitor C is discharged through inductor L_2 and capacitor C_0.

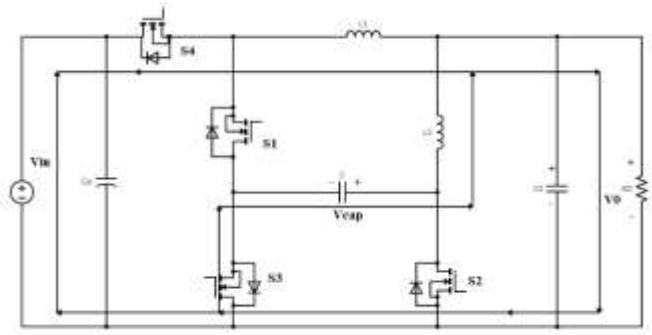

Figure 4 Status - I

Thus the inductor voltages in L_1 and L_2 are attained as

$$V_{L1} = V_{in} - V_0 \quad (3.1)$$
$$V_{L2} = V_{Cap} - V_0 \quad (3.2)$$

STATUS II ($t_1 \le t \le t_2$)

During this time span, the switches S1 and S2 are turned ON, while switches S3 and S4 are turned OFF, by means of applying the gate pulses to the appropriate switches. The inductor L_1 is demagnetized to capacitors C and C_0. The inductor energy stored in L_2 is released to capacitor C_0, which provides energy to the load. Therefore, the inductor voltages can be expressed as

$$V_{L1} = -V_0 - V_{Cap} \quad (3.3)$$
$$V_{L2} = -V_0 \quad (3.4)$$

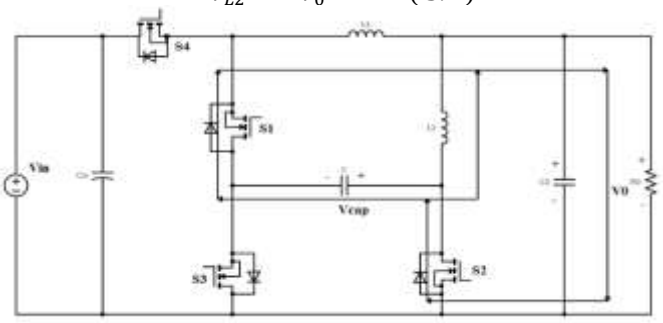

Figure 5 Status - II

Applying the technique of voltage-second (V-S) balance on the inductors L_1 and L_2, we obtain,

$$\langle V_{L1} \rangle = \int_0^{DT_s} (V_{in} - V_0)dt + \int_{DT_S}^{T_s} (-V_0 - V_{Cap})dt = 0 \quad (3.5)$$
$$\langle V_{L2} \rangle = \int_0^{DT_s} (V_{Cap} - V_0)dt + \int_{DT_S}^{T_s} (-V_0)dt = 0 \quad (3.6)$$

Hence, the voltage gain of step-down under continuous conduction mode specified by

$$G_{CCM(step-down)} = \frac{V_0}{V_{in}} = D^2 \quad (3.7)$$

If the inductors are operated under boundary condition mode (BCM), then the capacitors Cap and C_0 currents are expressed as

$$i_{Cap} = \{-I_{L2} \quad 0 \le t \le DT_S$$
$$i_{Cap} = \{I_{L1} \quad DT_S \le tT_s \quad (3.8)$$

The current of the capacitor C_0 is $I_{L1} + I_{L2} - I_0$. Applying the technique of A-S (ampere-second) balance on the capacitors, Cap and C_0,

$$\langle i_{Cap} \rangle = 0 = \frac{-DT_s I_{L2} + (1-D)T_S I_{L1}}{T_S} \Longrightarrow I_{L1} = \frac{D}{(1-D)} I_{L2} \quad (3.9)$$
$$\langle i_{Cap} \rangle = 0 \Longrightarrow I_{L1} + I_{L2} - I_0 \quad (3.10)$$

Therefore, the average currents of the inductors are

$$I_{L1} = DI_0 \quad (3.11)$$
$$I_{L2} = (1-D)I_0 \quad (3.12)$$

Current ripples of the inductors L_1 and L_2 can be attained as from the integral form of the current expressions of the inductors L_1 as well as L_2.

$$i_{L1}(DT_S) = i_{L1}(0) + \frac{1}{L_1}\int_0^{DT_S} V_{L1}(t)dt \Longrightarrow \Delta i_{L1} = \frac{D(V_{in}-V_0)}{L_1 f_{SW}} \quad (3.13)$$
$$i_{L2}(DT_S) = i_{L2}(0) + \frac{1}{L_2}\int_0^{DT_S} V_{L2}(t)dt \Longrightarrow \Delta i_{L2} = \frac{D(V_{Cap}-V_0)}{L_2 f_{SW}} \quad (3.14)$$

Express the inductor values as

$$I_{L1} \ge \frac{1}{2}\Delta i_{L1}$$
$$I_{L2} \ge \frac{1}{2}\Delta i_{L2}$$

Determine the value of L_1,

$$DI_0 \ge \frac{D(V_{in} - V_0)}{2L_1 f_{SW}}$$

where

$$I_0 = \frac{V_0}{R_0}; \frac{V_{Cap}}{V_{in}} = \frac{V_0}{V_{Cap}} = D$$

The expression becomes

$$D\frac{V_0}{R_0} = \frac{D(V_{in} - V_0)}{2L_1 f_{SW}}$$

Similarly, for the inductor value L_2,

$$(1-D)I_0 \ge \frac{D(V_{Cap} - V_0)}{2L_2 f_{SW}}$$
$$\frac{(1-D)V_0}{R_0} \ge \frac{D(V_{Cap} - V_0)}{2L_2 f_{SW}}$$

After simplification of the above Equations, the least possible values of inductors can be expressed as

$$L_1 \ge \frac{(1-D^2)R_0}{2D^2 f_{SW}} \quad (3.15)$$
$$L_2 \ge \frac{R_0}{2f_{SW}} \quad (3.16)$$

STEP – UP OPERATION

The circuit of proposed topology in step-up operation is illustrated in Figure 6; Here, S1 and S2 act as control switches and S3 and S4 are synchronous rectifiers. It operates under two statuses based on the triggering of the corresponding switches.

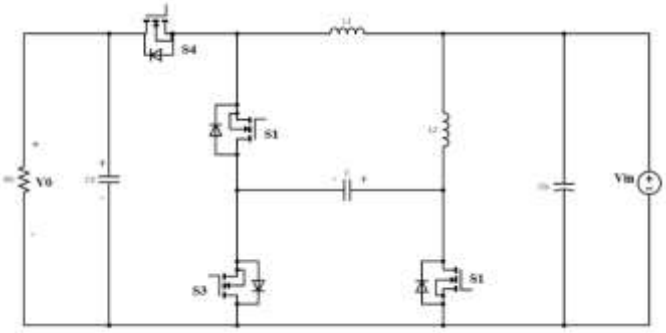

Figure 6 Step – Up Operation

STATUS – I ($t_0 \le t \le t_1$)

During this time span, the switches S_1 and S_2 are turned ON, while the switches S_3 and S_4 turned OFF at the same time by means of applying the gate pulses to the appropriate switches. The energy from the low-voltage end, which is the input voltage V_{in}, is transferred on the way to the inductor L_2. Inductor L_1 is magnetized by the input DC source V_{in} and the energy stored in capacitor C. The stored energy in the capacitor C_0 is released to the load, R_0.

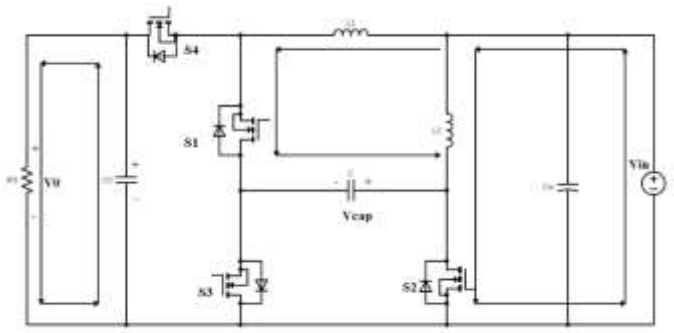

Figure 7 Status – I

Hence the voltages across the inductors L_1 and L_2 are expressed as

$$V_{L1} = V_{in} + V_{Cap} \quad (3.17)$$
$$V_{L2} = V_{in} \quad (3.18)$$

STATUS II ($t_1 \le t \le t_2$)

During this time span, the switches S_1 and S_2 are turned OFF, while switches S_3 and S_4 turned ON at the same time by means of applying the gate pulses to the appropriate switches. The capacitor C is charged by the input supply, V_{in}, and the energy stored in inductor L_2. Capacitor C_0 is also charged by the input supply, V_{in}, and the energy stored in inductor L_1.

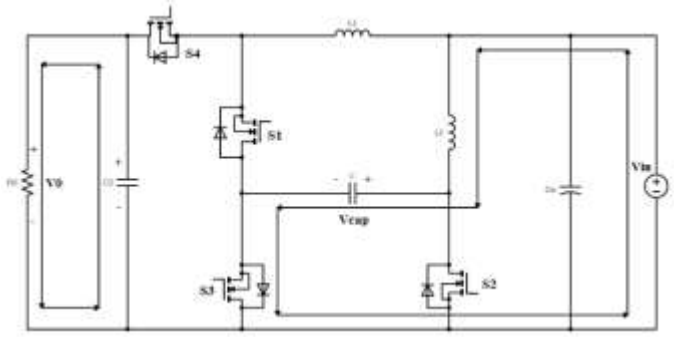

Figure 8 Status - II

The inductor voltages across L1 and L2 are expressed as

$$V_{L1} = V_{in} - V_0 \quad (3.19)$$
$$V_{L2} = V_{in} - V_{Cap} \quad (3.20)$$

According to the voltage-second (V-S) balance technique applied to the inductors, its further generalization produces the Equation for step-up gain in continuous conduction mode (CCM) as exemplified by the following expressions:

$$\int_0^{DT_S}(V_{in} + V_{Cap})dt + \int_{DT_S}^{T_S}(V_{in} - V_0)dt = 0 \quad (3.21)$$
$$\int_0^{DT_S} V_{in}dt + \int_{DT_S}^{T_S}(V_{in} - V_{Cap})dt = 0 \quad (3.22)$$
$$G_{CCM(step-up)} = \frac{V_0}{V_{in}} = \frac{1}{(1-D)^2} \quad (3.23)$$

The C and C_0 capacitor currents are expressed as

$$i_{Cap} = \{-I_{L1} \quad 0 \le t \le DT_S$$
$$i_{Cap} = \{I_{L2} \quad DT_S \le t \le T_S \quad (3.24)$$
$$i_{C_0} = \{-I_0 \quad 0 \le t \le DT_S$$
$$i_{C_0} = \{I_{L1} - I_0 \quad DT_S \le t \le T_S \quad (3.25)$$

By using the ampere-second balance principle on C and C_0,

$$\langle i_{Cap} \rangle = 0 = \frac{-DT_S I_{L1} + (1-D)T_S I_{L2}}{T_S} \Longrightarrow I_{L2} = \frac{D}{(1-D)} I_{L1} \quad (3.26)$$
$$\langle i_{C_0} \rangle = 0 = I_{L1} = \frac{1}{(1-D)} I_0 \quad (3.27)$$
$$I_{L2} = \frac{D}{(1-D)^2} I_0 \quad (3.28)$$

The expression for the inductor current ripples in L_1 and L_2 are written as

$$i_{L1}(DT_S) = i_{L1}(0) + \frac{1}{L_1}\int_0^{DT_S} V_{L1}(t)dt \Longrightarrow \Delta i_{L1} = \frac{D(V_{in}+V_{Cap})}{L_1 f_{SW}} \quad (3.29)$$
$$i_{L2}(DT_S) = i_{L2}(0) + \frac{1}{L_2}\int_0^{DT_S} V_{L2}(t)dt \Longrightarrow \Delta i_{L2} = \frac{DV_{in}}{L_2 f_{SW}} \quad (3.30)$$

The converter operates under CCM, when the average value of an inductor is more than half of its current ripples. The inductor values based on its ripples are expressed as

$$I_{L1} \ge \frac{1}{2}\Delta i_{L1}$$
$$I_{L2} \ge \frac{1}{2}\Delta i_{L2}$$

For determining the value of L_1,

$$\frac{I_0}{1-D} \ge \frac{D(V_{in} + V_{Cap})}{2L_1 f_{SW}}$$

where

$$I_0 = \frac{V_0}{R_0}; \frac{V_{Cap}}{V_{in}} = \frac{V_0}{V_{Cap}} = \frac{1}{1-D}$$

The expression becomes

$$\frac{V_0}{R_0(1-D)} = \frac{D(2-D)V_{Cap}}{2L_1 f_{SW}}$$

Similarly, for the inductor value L_2,

$$\frac{DI_0}{(1-D)^2} \ge \frac{DV_{in}}{2L_2 f_{SW}}$$
$$\frac{V_0}{R_0(1-D)^2} \ge \frac{V_{in}}{2L_2 f_{SW}}$$

After simplification of the above expressions, the least possible values of inductors can be found as

$$L_1 \ge \frac{D(2-D)(1-D)^2 R_0}{2f_{SW}} \quad (3.31)$$
$$L_2 \ge \frac{(1-D)^4 R_0}{2f_{SW}} \quad (3.32)$$

If the values of the inductors are less than the above expression, then the converter will face the boundary condition or even the discontinuous conduction mode.

4. DESIGN CONSIDERATION

DESIGN CONSIDERTION OF THE PROPOSED SYSTEM

INDUCTOR VALUE

The primary specifications for designing a power converter system are input voltage V_{in} and output voltage V_0. Inductors play a crucial role in energy storage, current regulation and voltage conversion.

In this system, two inductors L1 and L2 are used for better performance of the converter.

Here, for Step-down and step-up operation, from the equation (3.15) & (3.32),

$$L_1 \ge \frac{(1-D^2)R_0}{2D^2 f_{SW}} \sim 420\ \mu H$$
$$L_2 \ge \frac{(1-D)^4 R_0}{2f_{SW}} \sim 520\ \mu H$$

Where, D = Duty Cycle
R_0 = Internal Resistance
f_{SW} =Switching Frequency

DUTY CYCLE

The duty cycle of a converter refers to the ratio of the time a switch is in the "ON" state to the total time of one switching period.

It is a key parameter that control the converter's output voltage, power flow direction and operating modes.

The voltage gains for buck operation and boost operation of the converter in the proposed topology from the equations (3.7) & (3.23) are as follows,

$$Step - Down\ mode: D = \sqrt{\frac{V_{in}}{V_o}} \sim 0.2$$

$$Step - Up\ mode: D = 1 - \sqrt{\frac{V_0}{V_{in}}} \sim 0.6$$

Where, V_{in} = Input Voltage
V_0 = Output Voltage

OUTPUT CAPACITOR

The output capacitor in the dual-active bridge must be designed to handle the ripple. The capacitor current is the difference between the current IHB2 and the output current I_{out}, also called I_{out}. The best output current I_{out} is obtained by Pout / V_0. From the difference between I_{out} and IHB2 the charge ΔQ can be obtained. Afterwards, the required capacitance can be calculated for a maximum allowed ripple voltage.

$$C_0 = \frac{\Delta Q}{V_{ripple}} = 470\ \mu F$$

5. SIMULATION SPECIFICATIONS

STEP-DOWN OPERATION

Table 2 Simulation Parameter for Step-Down Operation

PARAMETERS	SPECIFICATIONS
INPUT VOLTAGE	215V
OUTPUT VOLTAGE	24V
OUTPUT CURRENT	2.7A
DUTY CYCLE	20%
INDUCTOR L_1, L_2	420 μH, 520 μH
OUTPUT CAPACITOR	470 μF

STEP-UP OPERATION

TABLE 3 Simulation Parameter for Step-Up Operation

PARAMETERS	SPECIFICATIONS
INPUT VOLTAGE	24V
OUTPUT VOLTAGE	220V
OUTPUT CURRENT	0.7A
DUTY CYCLE	60%
INDUCTOR L_1, L_2	420 μH, 520 μH
OUTPUT CAPACITOR	470 μF

BATTERY SPECIFICATION

Table 4 Battery Specifications

PARAMETERS	SPECIFICATION
BATTERY TYPE	LEAD-ACID
VOLTAGE	24V
CURRENT	7.2Ah
TEMPERATURE	27℃
INITIAL CURRENT	2.25A

6. SIMULATION AND RESULTS

SIMULATION CIRCUIT

The simulation circuit of the proposed system is shown in figure 9. The simulation is done in MATLAB 2023A version with ode45 solver. The Discrete powergui with a value of 1 μs is used to run the simulation and visualize the results. The proposed converter is provided in open loop control for getting better performance.

In this circuit, there are two separate circuits are shown. It shows the bidirectional working of the converter. In the circuit, the above one shows the step-down operation of the power converter and the below one shows the step-up operation of the power converter.

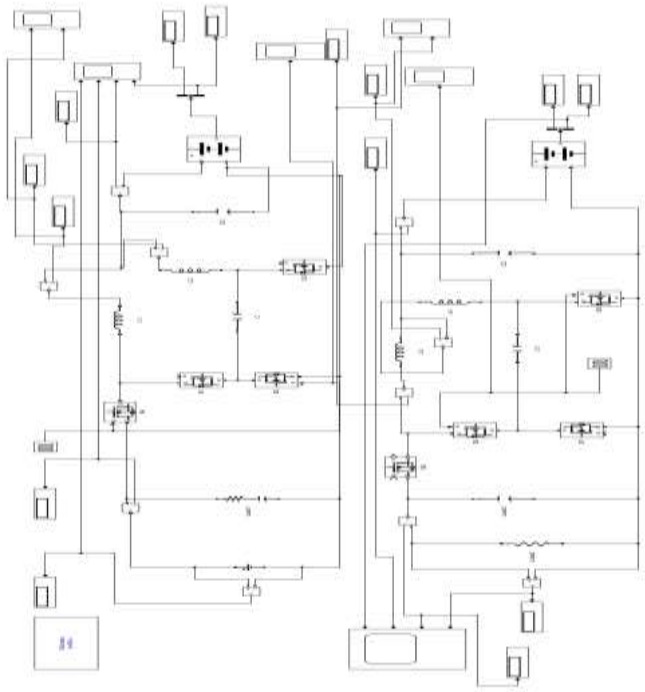

Figure 9 Simulation Diagram

POWER FLOW IN STEP-DOWN OPERATION

In the figure 10 shows the simulation circuit of the step-down operation of the bidirectional converter of the proposed system. In this circuit it shows the power flow from high voltage side (Eg. DC Grid) to the low voltage side.

This circuit is made for the charging purpose of the battery in the electric vehicle.

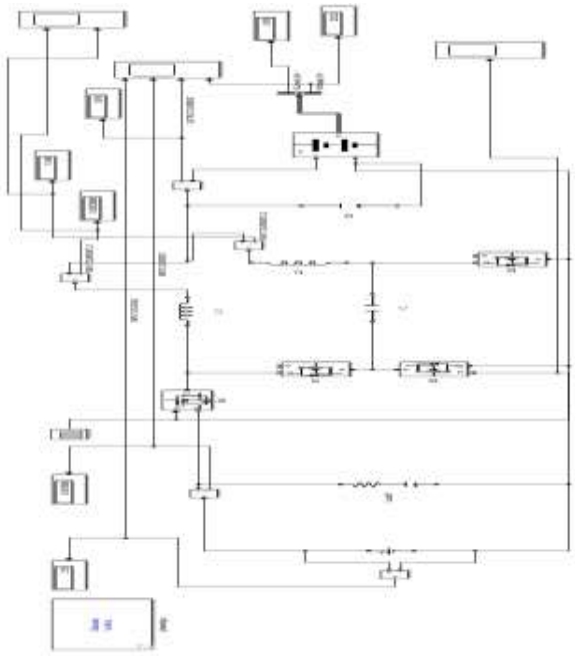

Figure 10 Step-Down Operation

SWITCHING PULSE

Switching pulse for the step-down operation is shown the figure 11. It shows the pulse for the switch S3 and S4 of the converter. This is for the switch turn ON and OFF time of the converter.

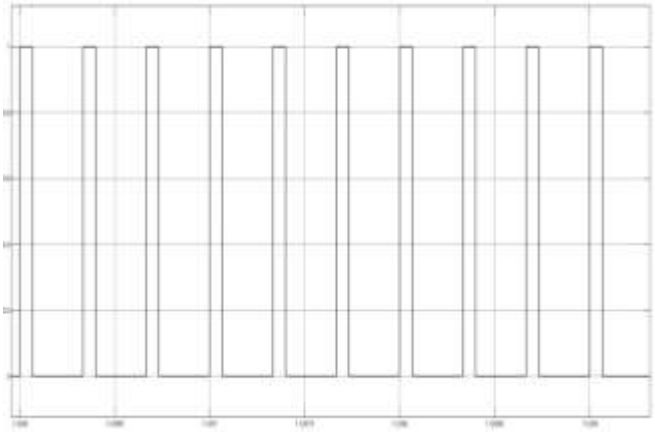

Figure 11 Switching pulse of Step-down Operation

OUTPUT WAVEFORM

From the simulation of the step-down operation, the results are displayed in the figure 12. It shows the waveforms of input voltage V_{in}, input current I_{in}, output voltage V_0 and output current I_0.

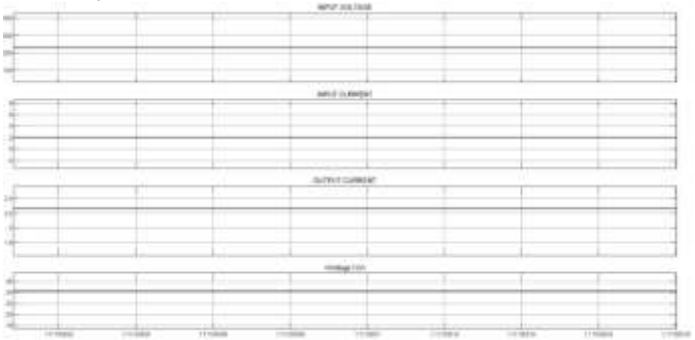

Figure 12 Input and Output Waveforms of Step-down Operation

POWER FLOW IN STEP-UP OPERATION

In the figure 13 shows the simulation circuit of the step-down operation of the bidirectional converter of the proposed system. In this circuit it shows the power flow from low voltage side (Eg. EV Battery) to the high voltage side.

This circuit is made for the discharging purpose of the battery in the electric vehicle.

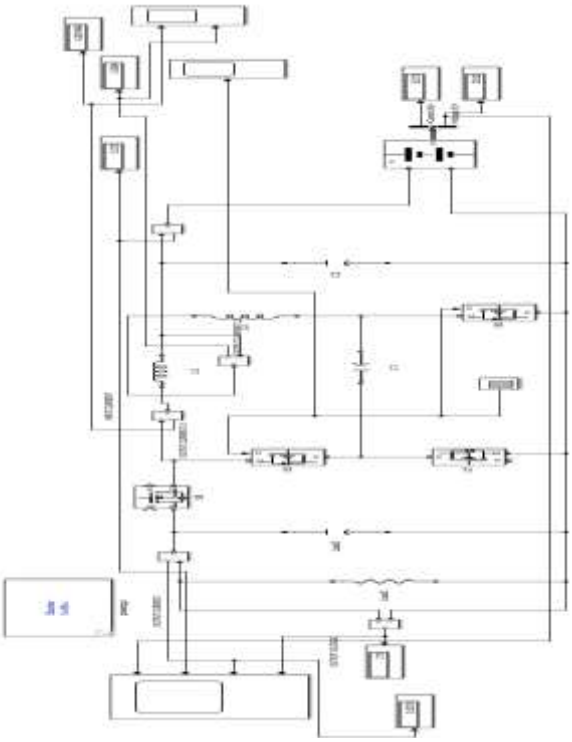

Figure 13 Step-Up Operation

SWITCHING PULSE

Switching pulse for the step-up operation is shown the figure 14. It shows the pulse for the switch S1 and S2 of the converter. This is for the switch turn ON and OFF time of the converter.

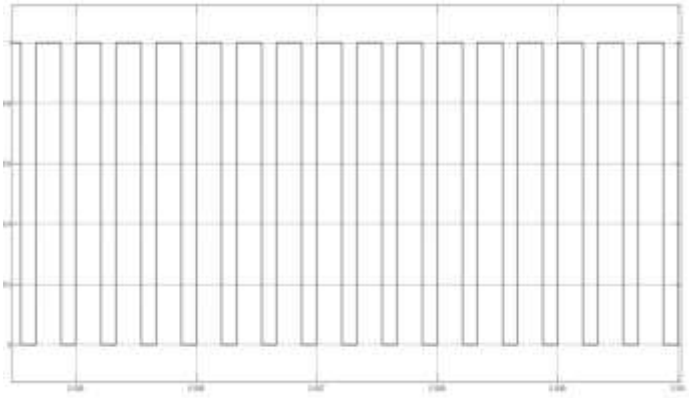

Figure 14 Switching Pulse of Step-Up Operation

OUTPUT WAVEFORM

From the simulation of the step-up operation, the results are displayed in the figure 15. It shows the waveforms of input voltage V_{in}, input current I_{in}, output voltage V_0 and output current I_0.

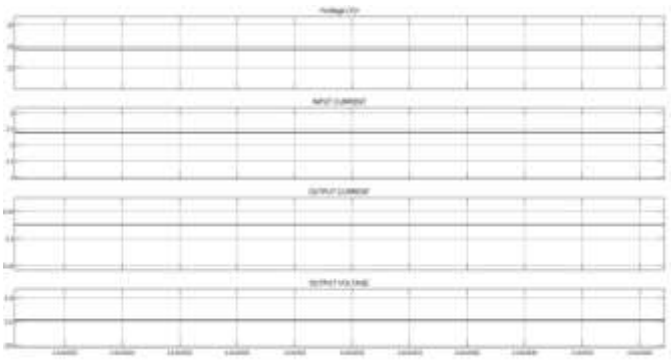

Figure 15 Input and Output Waveforms of Step-up Operation

7. HARDWARE IMPLEMENTATION

HARDWARE SETUP

The Non-Isolated Bidirectional DC-DC Converter prototype is tested for battery charging and discharging as shown in the figure 16.

FIGURE 16 Hardware Setup

GATE DRIVE CIRCUIT

Figure 17 shows the gate drive circuit of the bidirectional DC-DC converter. It is used for giving the gate pulse for the MOSFET switch in the converter.

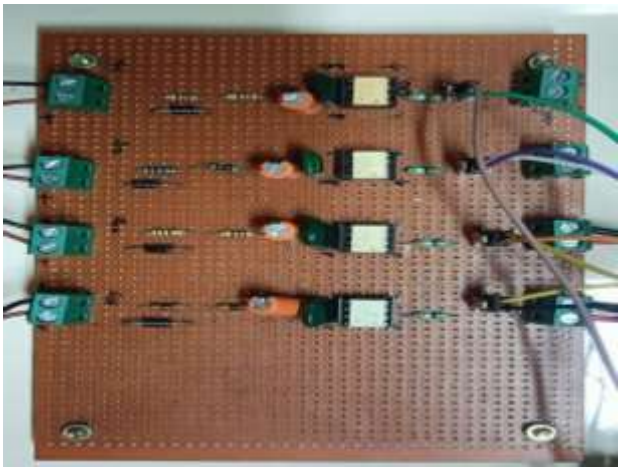

Figure 17 Gate Drive Circuit

HYBRID NON-ISOLATED BIDIRECTIONAL DC-DC CONVERTER

Figure 18 shows the Non-Isolated Bidirectional DC-DC converter circuit. It works in both the direction of input and output sides of the converter.

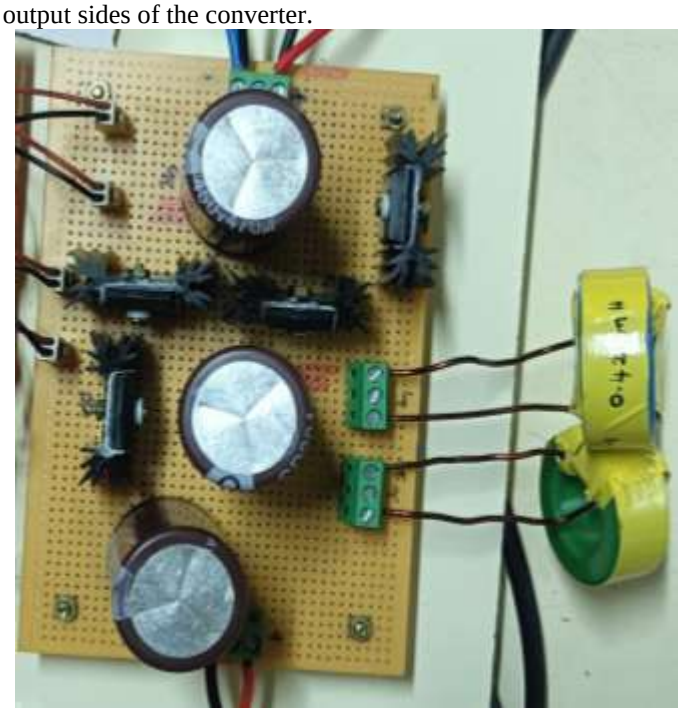

Figure 18 Hybrid Non-Isolated Bidirectional DC-DC Converter

HARDWARE OUTPUT WAVEFORMS

STEP-DOWN OPERATION OUTPUT

In step-down operation, the battery gets charging with high current. Figure 19 and 20 shows the gate pulse output and output voltage of the converter.

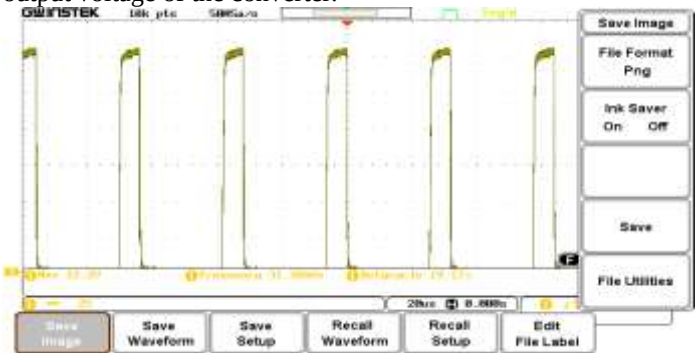

Figure 19 Step-down Operation Gate Pulse Output Waveform

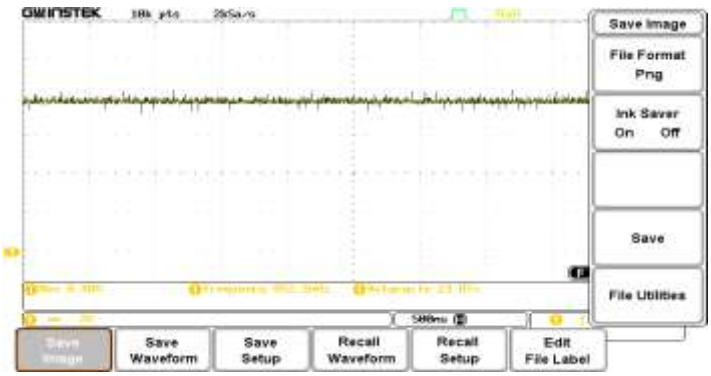

Figure 20 Step-down Operation Output Voltage Waveform

Here, the input voltage is 30V and the output voltage is getting as 8.4V. The duty cycle of the switching operation is 20% for the charging condition.

STEP-UP OPERATION OUTPUT WAVEFORMS

In step-up operation, the battery output is boosted up with the converter and it is integrated with grid or used for the various applications. Figure 21 and 22 shows the gate pulse output and output voltage of the converter.

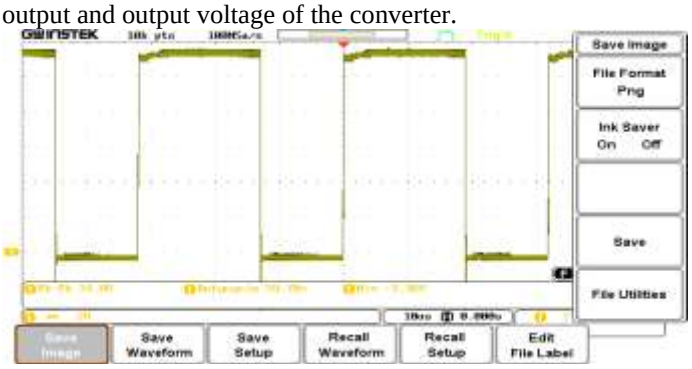

Figure 21 Step-up Operation Gate Pulse Output Waveform

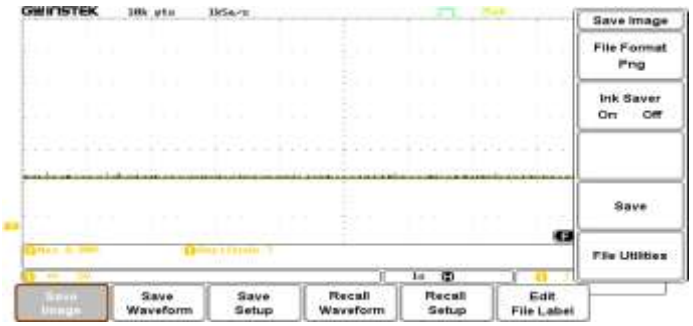

Figure 22 Step-up Operation Output Voltage Waveform

Here, the input voltage is 2.5V and the output voltage is getting as 8V. The duty cycle of the switching operation is 60% for the charging condition.

HARDWARE SPECIFICATIONS

GATE DRIVE CIRCUIT COMPONENTS

Table 5 Gate Drive Circuit Components

COMPONENTS	SPECIFICATIONS
8-pin IC	TLP250/TLP250H
Polarised Capacitor	100µF
Unpolarised Capacitor	100nF
Diode	FR107
Resistors	390Ω,10Ω

CONVERTER CIRCUIT COMPONENTS

Table 6 Converter Circuit Components

COMPONENTS	SPECIFICATIONS
MOSFET Switches	IRF450
Inductor L_1	420µH
Inductor L_2	520µH
Capacitor C	470µF
Capacitor C_0 & C_{in}	470µF

Here, in this paper the converter is also capable for input voltage of 215V as DC supply. The Battery specification is up to 96V 7.2Ah.

CONCLUSION

This project successfully demonstrates the design of hybrid non-isolated bidirectional DC-DC converter. The suggested system incorporates modern power conversion methods to guarantee effective and bidirectional power flow, which is necessary for high voltage gain, bidirectional battery charging, and contemporary EV systems.

When compared to traditional converters, the suggested architecture yields a large voltage gain during both step-up and step-down operations. The input current splits between the two inductors during step-up operation, increasing the voltage gain. The efficiency is increased because the total of the two inductor currents produces a high output current as a result of the switches' synchronous rectification during step-down operation. As a result, battery charging applications with a lower output voltage and a higher current are best suited for the suggested design.

Furthermore, incorporating cutting-edge control techniques like AI-based adaptive or predictive control may improve the system's dynamic reaction, stability, and efficiency even more. In addition to addressing greater voltage levels and lowering switching losses, investigating multilayer converter topologies may make them appropriate for a wider variety of EV applications. Battery life can be increased and state-of-charge management optimized with additional integration with Battery Management Systems (BMS). The sustainability of EV systems may also be improved by modifying the design to be compatible with renewable energy sources like solar and wind power. Finally, this study is expanding this technology for different EV configurations, such as heavy-vehicles, cars and two-wheelers, could increase its application.

REFERENCES

1. Benevieri. A, Carbone. L, Cosso. S, Gallione. F, and Hussain. S, "Multi-input bidirectional DC–DC converter for energy management in hybrid electrical vehicles applications," in Proc. 13th Int. Symp. Adv. Topics Electr. Eng. (ATEE), Mar. 2023, pp. 1–5
2. Chakraborty, S.; Reza, S.M.S.; Hasan, W. Design and analysis of hybrid solar-wind energy system using CUK & SEPIC converters for grid connected inverter application. In Proceedings of the 2015 IEEE 11th International Conference on Power Electronics and Drive Systems, Sydney, NSW, Australia, 9–12 June 2015; pp. 278–283.
3. Elsayad. N, Moradisizkoohi. H, and Mohammed. O. A, "A new hybrid structure of a bidirectional dc-dc converter with high conversion ratios for electric vehicles," IEEE Trans. Veh. Technol., vol. 69, no. 1, pp. 194–206, Jan. 2020.
4. Elsayad. N, Moradisizkoohi. H, and Mohammed. O. A, "Design and implementation of a new transformerless bidirectional dc-dc converter with wide conversion ratios," IEEE Trans. Ind. Electron., vol. 66, no. 9, pp. 7067–7077, Sep. 2019.
5. Guo J, Rodriguez R, Gareau J, Schumacher D, Alizadeh M, Azer P, Bauman J, Bilgin B, Emadi. A.A Comprehensive Analysis for High-Power Density, High-Efficiency 60kW Interleaved Boost Converter Design for Electrified Powertrains. IEEE Trans. Veh. Technol. 2020, pp. 69, 1.
6. Gupta. C and Das. M., "Multiphase interleaved DC–DC converter for fast charging application of electric vehicles," in

Proc. IEEE 16th Int. Conf. Compat., Power Electron., Power Eng. (CPE-POWERENG), Jun. 2022, pp. 1–6
7. Hamed Heydari-Doostabad, Terence O'Donnell, A Wide Range High Voltage Gain Bidirectional DC-DC Converter for V2G and G2V Hybrid EV Charger. IEEE Transactions On Industrial Electronics, 2021
8. Hirth. M. P, Gules. R and Illa Font. C. H, "A wide conversion ratio bidirectional modified SEPIC converter with nondissipative current snubber," IEEE J. Emerg. Sel. Top. Power Electron., vol. 9, no. 2, pp. 1350–1360, Apr. 2021.
9. Hosseini. S. H, Ghazi. R, and Heydari-Doostabad. H, "An extendable quadratic bidirectional dc-dc converter for V2G and G2V applications", IEEE Trans. Ind. Electron., vol. 68, no. 6, pp. 4859–4869, Jun. 2021.
10. Lai. C. M, Development of a Novel Bidirectional DC/DC Converter Topology with High Voltage Conversion Ratio for Electric Vehicles and DC-Microgrid. Energies 2016, 9, pp. 410.
11. Lin C.C, Wu. G, Yang L.-S. Study of a non-isolated bidirectional DC–DC converter. IET Power Electron.2013, 6, pp. 30–37.
12. Ma. C. T, Design and Implementation of a Bidirectional DC/DC Converter for BESS Operations. Proc. IMECS 2017, 2, pp. 666–671.
13. Mahafzah, K.A.; Obeidat, M.A.; Al-Shetwi, A.Q.; Ustun, T.S. A Novel Synchronized Multiple Output DC-DC Converter Based on Hybrid Flyback-Cuk Topologies. Batteries 2022, 8, pp. 93.
14. Mahafzah, K.A.; Rababah, H.A. A novel step-up/step-down DC-DC converter based on flyback and SEPIC topologies with improved voltage gain. Int. J. Power Electron. Drive Syst. (IJPEDS) 2023, 14, pp. 898–908.
15. NarasimhaRaju. B. L, Reddy. U. R, Dogga. R, Design and analysis of voltage clamped bidirectional DC–DCconverter for energy storage applications. J. Eng., 2018, pp. 367–374.
16. Ravi. D, Mallikarjuna Reddy. B, and Samuel. P. (2018). Bidirectional DC To DC Converters: An Overview of Various Topologies, Switching Schemes and Control Techniques.
17. Reddy. P. L. S. K, Obulesu. Y. P, Singirikonda. S, Al Harthi. M, Alzaidi. M. S, Ghoneim. S. S. M, A Non-Isolated Hybrid Zeta Converter with a High Voltage Gain and Reduced Size of Components, Electronics 2022, 11, pp. 483.
18. Savio. D.A, Juliet. A.V, Bharatiraja. C, Padmanaban. S, Hossain. E, Blaabjerg. F, Photovoltaic Integrated Hybrid Microgrid Structured Electric Vehicle Charging Station and Its Energy Management Approach. Energies 2019, 12, pp. 168.
19. Zhang. H, Chen. Y, Park. S. J, Kim. D. H, A Family of Bidirectional DC–DC Converters for Battery Storage System with High Voltage Gain. Energies 2019, 12, pp. 1289.
20. Zhang. Y, Gao. Y, Li. J, Sumner. M, Wang. P, Zhou. L, High Ratio Bidirectional DC-DC Converter with a Synchronous Rectification H-Bridge for Hybrid Energy Sources Electric Vehicles. J. Power Electron. 2016, 16, pp. 2035–2044.